

Dense matter in strong magnetic fields

Monika Sinha

Institute for Theoretical Physics, J. W. Goethe-University, D-60438 Frankfurt-Main, Germany
 Indian Institute of Technology Rajasthan, Jodhpur 342011, Rajasthan, India

Abstract. Compact stars having strong magnetic fields (magnetars) have been observationally determined to have surface magnetic fields of order of $10^{14} - 10^{15}$ G, the implied internal field strength being several orders larger. We study the equation of state and composition of hypernuclear matter and quark matter - two forms of dense matter in strong magnetic fields. We find that the magnetic field has substantial influence on the properties of hypernuclear matter and quark matter for magnetic field $B \geq 10^{17}$ G and $B \geq 10^{18}$ G respectively. In particular the matter properties become anisotropic. Moreover, above a critical field B_{cr} , both hypernuclear and quark matter show instability, although the values of B_{cr} are different for two kinds of matter.

1. Introduction

Soft γ -ray repeaters and anomalous X-ray pulsars are commonly believed to be magnetars - the compact stars with surface magnetic fields $B_s \sim 10^{14} - 10^{15}$ G. The interpretation of astrophysical observations of magnetars requires good knowledge of the properties of dense matter in the presence of large magnetic fields. The properties of dense matter inside the compact objects is poorly known due to lack of the proper knowledge of strong interactions that are relevant at densities of interest. As a consequence, many phenomenological models of dense matter have been proposed over the years. The models of dense matter can tentatively be divided into two broad classes: one class includes matter made of ordinary hadronic matter; the second class is deconfined quark-gluon state with about equal number of up, down and strange quarks, known as the strange quark matter (SQM). In both cases the underlying constituent particles are fermions which are interacting via exchange of bosons. Fermions in strong magnetic field experience two well-known quantum mechanical effects: the Pauli paramagnetism and the Landau diamagnetism. The first is due to the interaction of the spin of the fermion with the magnetic field and therefore, is relevant for both charged and uncharged fermions. The second effect is relevant only for charged fermions, and is particularly strong for light particles, which in the case of compact stars are the leptons.

Since one can not exclude the possibility of a density dependent field profile which is favorable for local magnetostatic equilibrium inside a star, we consider the hyperonic matter under the influence of density dependent magnetic field. Among many effective phenomenological models to study the quark matter, the MIT bag model [4] and the Nambu-Jona-Lasinio (NJL) model [5, 6] are the most popular ones. However, the NJL model does not account for confinement property of QCD, while the bag model cannot account for the chiral symmetry breaking, although it is built in a manner as to confine through an *ad hoc* bag pressure. We will base our discussion of quark matter in strong magnetic field and at nonzero temperature on a model

originally introduced by Dey *et. al.* [7]. In this model quark masses are density dependent ensuring chiral symmetry restoration at high density and the quarks interact among themselves via the Richardson potential (RP) [8] in which asymptotic freedom and confinement are built in. In the next section we discuss the general effect of magnetic field on fermionic matter. In Sec. 3 we discuss the results concerning the equation of state (EoS) of hypernuclear and quark matter in strong magnetic fields. Our conclusions are presented in Sec. 4.

2. Magnetized matter

In the presence of a magnetic field the motion of charged fermions is Landau quantized in the plane perpendicular to the direction of the magnetic field. If the field direction is assumed to be the direction of z -axis the single particle energy of a charged particle with mass m in the n -th Landau level is $\epsilon_n = \sqrt{p_z^2 + m^2 + 2ne|Q|B}$, p_z being the momentum parallel to the field (which is in the z direction of Cartesian system of coordinates) and Q being the charge of the particle in units of proton charge. Evidently, the momentum of a particle in the x - y plane is quantized. The phase space sampling for such a particle is therefore modified according to the rule (the spin degeneracy is included)

$$2 \int_0^{p_F} d^3p \longrightarrow e|Q|B \sum_{n=0}^{n_{max}} (2 - \delta_{n,0}) \int_{-p_{F,n}}^{p_{F,n}} dp_z \int_0^{2\pi} d\phi, \quad (1)$$

where ϕ is the azimuthal angle and $p_{F,n} = \sqrt{p_F^2 - 2ne|Q|B}$ with p_F being the Fermi momentum.

In the presence of electromagnetic field the energy momentum tensor of a fermionic system in the rest frame of matter is $T^{\mu\nu} = T_m^{\mu\nu} + T_f^{\mu\nu}$, where the matter part of energy momentum tensor is

$$T_m^{\mu\nu} = \begin{bmatrix} \epsilon_m & 0 & 0 & 0 \\ 0 & P_m - MB & 0 & 0 \\ 0 & 0 & P_m - MB & 0 \\ 0 & 0 & 0 & P_m \end{bmatrix}, \quad (2)$$

and in the absence of electric field the field part of the energy momentum tensor is

$$T_f^{\mu\nu} = \frac{B^2}{8\pi} \begin{bmatrix} 1 & 0 & 0 & 0 \\ 0 & 1 & 0 & 0 \\ 0 & 0 & 1 & 0 \\ 0 & 0 & 0 & -1 \end{bmatrix}. \quad (3)$$

The matter energy density ϵ_m is obtained by integrating the single particle energies of each species over appropriate phase space volume and then adding their contributions. The thermodynamic pressure at zero temperature is $P_m = \sum_i \mu_i n_i - \epsilon_m$, where μ and n are chemical potential and number density of corresponding species. The total energy density of the system is given by the sum of the matter and field contributions $\epsilon = \epsilon_m + B^2/8\pi$. It is clear from Eqs. (2) and (3) that the presence of magnetic field makes the pressure anisotropic: the pressure in the perpendicular to the magnetic field direction is $P_{\perp} = P_m - MB + B^2/8\pi$, whereas the pressure in the direction parallel to the magnetic field is $P_{\parallel} = P_m - B^2/8\pi$.

We study the hyperonic matter in the presence of strong magnetic field within the nonlinear Boguta-Bodmer-Walecka model [9, 10]. The model is described in detail in Ref. [11]. The field profile has been adopted according to [12]

$$B \left(\frac{n_b}{n_0} \right) = B_s + B_c \left\{ 1 - \exp \left[-\beta \left(\frac{n_b}{n_0} \right)^{\gamma} \right] \right\}. \quad (4)$$

The parameters β and γ control the relaxation from the central value B_c to the asymptotic value at the surface B_s . Here n_b is the baryon number density, n_0 is the normal nuclear matter density.

In the case of quark matter at finite temperature, we consider matter composed of u , d and s quarks which interact via the Richardson potential [8]

$$V(q^2) = -\frac{4}{9} \frac{\pi}{\ln[1 + (q^2 + m_g^2)/\Lambda^2]} \frac{1}{(q^2 + m_g^2)}, \quad (5)$$

where m_g is gluon mass and Λ is a scale parameter. The finite gluon mass is responsible for screening in medium and is related to the screening length D via

$$m_g^2 = D^{-2} = \frac{2\alpha_0}{\pi} \sum_{i=u,d,s} k_F^i \mu_i^*, \quad (6)$$

where α_0 is the perturbative quark gluon coupling, $\mu_i^* = \sqrt{(k_F^i)^2 + m_i^2}$ is the Fermi energy (the chemical potential at zero temperature), k_F^i is the Fermi momentum and m_i the quark mass. In this model the quark masses vary with density as [7]

$$m_i = M_i + M_q \operatorname{sech}\left(\nu \frac{n_b}{n_0}\right), \quad i = u, d, s, \quad (7)$$

where ν is a parameter. At large n_b the quark mass m_i falls off from its constituent value M_q to its current value M_i .

The kinetic part of the energy density for a particular quark flavor in the presence of magnetic field and at non-zero temperature is given by

$$\varepsilon_{kin} = \frac{3}{(2\pi)^3} e|Q|B \sum_{n=0}^{\infty} (2 - \delta_{n,0}) \int_0^{2\pi} d\phi \int_{-\infty}^{\infty} f(\epsilon) \epsilon dk_z, \quad (8)$$

where $f(\epsilon)$ is Fermi distribution function. The potential part of the energy density due to interaction between the flavors i and j is given by

$$\begin{aligned} \varepsilon_{pot}^{ij} &= \frac{e^2 |Q_i| |Q_j|}{(2\pi)^5} B^2 \sum_{n_i} \sum_{n_j} (2 - \delta_{n_i,0}) (2 - \delta_{n_j,0}) \\ &\int_0^{2\pi} d\phi_i \int_0^{2\pi} d\phi_j \int_{-\infty}^{\infty} dk_z^i \int_{-\infty}^{\infty} dk_z^j f(\epsilon_i) f(\epsilon_j) NV(q^2) S, \end{aligned} \quad (9)$$

where

$$N = \frac{(\epsilon_i + m_i)(\epsilon_j + m_j)}{4\epsilon_i \epsilon_j}, \quad S = 1 + \frac{k_i^2 k_j^2}{(\epsilon_i + m_i)^2 (\epsilon_j + m_j)^2} + \frac{2\mathbf{k}_i \cdot \mathbf{k}_j}{(\epsilon_i + m_i)(\epsilon_j + m_j)}.$$

The matter pressure is then given by

$$P_m = \sum_i \mu_i n_i + Ts - \varepsilon, \quad (10)$$

where T is the temperature, s is the entropy density and ε is the sum of the kinetic and potential energies. For further details see Ref. [13].

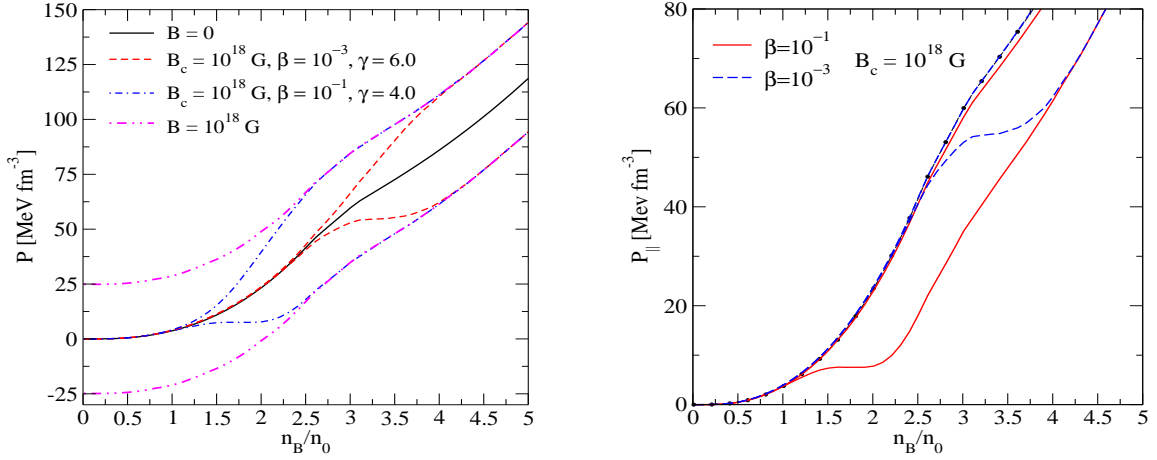


Figure 1. *Left panel (a):* Variation of total pressure as a function of normalized baryon number density for fixed magnetic fields $B_c = 0$ (solid line) and $B_c = 10^{18}$ G with several field profiles, $\beta = 10^{-3}$, $\gamma = 6$ (dashed lines), $\beta = 10^{-1}$, $\gamma = 4$ (dashed-dotted lines), and $\beta \rightarrow \infty$, *i.e.*, $B_c = \text{constant}$ (dashed-double-dotted lines). For each pair of curves the upper branch is for P_{\perp} and the lower branch for P_{\parallel} . *Right panel (b):* Dependence of P_{\parallel} on the normalized baryon number density for different magnetic field profiles and $B_c = 10^{18}$ G. The dots show the reference case $B_c = 0$. The solid and dashed lines correspond to $\beta = 0.1$ and 0.001 , respectively. For each β we choose a pair of γ 's; in the first case we have $\gamma = 1$ and $\gamma = 4$, whereas in the second case $\gamma = 1$ and $\gamma = 6$.

3. Results

Fig. 1a shows the EoS of hyperonic matter in the cases of no magnetic field, constant field as well as for fields with various density profiles. For nonzero magnetic fields the pressure splits into parallel and perpendicular components showing anisotropy which arises from the magnetic field contribution. From Fig. 1a it is also evident that there is an onset of instability for some field profiles due to P_{\parallel} component of the pressure. This is shown in Fig. 1b in a more systematic manner. It is clear that for a given value of β the corresponding EoS becomes softer as γ is increased. Consequently, beyond a certain critical value of γ and in a certain density regime P_{\parallel} ceases to increase and subsequently decreases with further increase in n_b . This implies that matter becomes unstable above that value of density for that particular B_c and magnetic field profile. For comparison we also show results for each β with the minimum value of γ taken to be 1. Note that the maximum value of γ is taken such that P_{\parallel} forms a plateau as a function of n_b .

The instability arises due to the negative contribution from the field energy density (pressure) to the net pressure of magnetized matter in the direction of the magnetic field. Since for any particular B_c and magnetic profile the field strength increases with the increase of n_b more negative contribution is added to P_{\parallel} with the increase of n_b . Consequently, at a certain density, P_{\parallel} ceases to increase and then decreases with the increase of n_b .

We turn now to the problem of quark matter in strong magnetic fields and we focus below on the effect of the RP model on the magnetized SQM at finite temperature. Our investigation shows that the results are not sensitive to the temperature in the range relevant to the physics of compact stars. Hence, we report here results with a fixed temperature $T = 20$ MeV. In Fig. 2a we show the EoS of SQM for the RP model and the bag model. Magnetic field introduces some oscillations in the pressure with density; in each case the increase of pressure after a

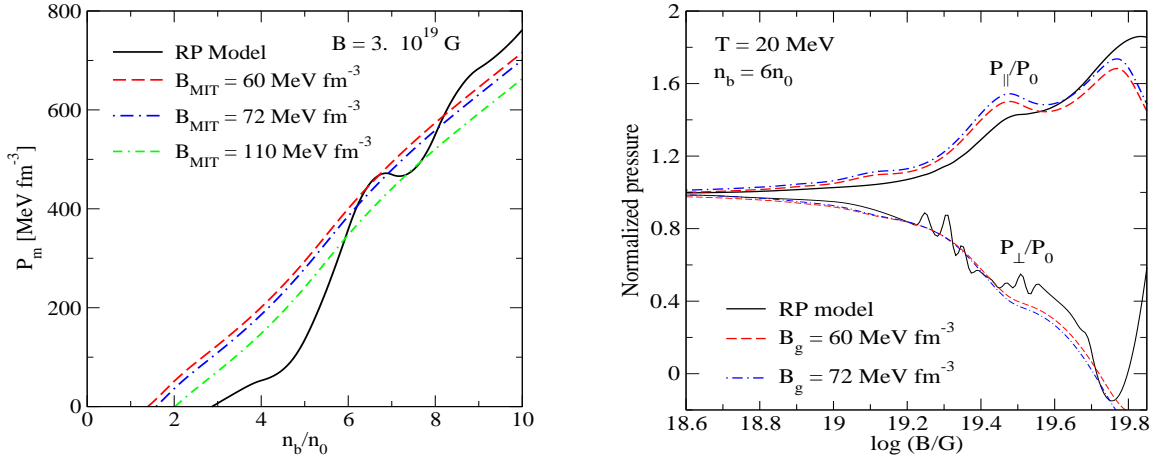


Figure 2. *Left panel* (a): Dependence of the thermodynamic pressure P_m on the normalized baryon number density at $T = 20 \text{ MeV}$ for $B = 3 \times 10^{19} \text{ G}$. The pressure is shown for the RP model (solid), for the MIT bag model with $B_{\text{MIT}} = 60 \text{ MeV fm}^{-3}$ (dashed), $B_{\text{MIT}} = 72 \text{ MeV fm}^{-3}$ (dash-dotted) and $B_{\text{MIT}} = 110 \text{ MeV fm}^{-3}$ (double-dash-dotted). *Right panel* (b): Dependence of the normalized pressure components that are parallel and perpendicular to the magnetic field on the strength of the magnetic field at $n_b = 6n_0$ and $T = 20 \text{ MeV}$ for various models. The upper three curves correspond to the parallel pressure, the lower three - to the perpendicular pressure.

plateau is caused by the opening of a new Landau level. The oscillations are much stronger in the RP model and this can be traced back to the momentum dependence of the potential. The major contribution comes from the static gluon propagator part of the potential, while the logarithmic factor in the potential depends weakly on momentum. Note that at a certain density the pressure has a plateau and slight negative downturn, which can be interpreted as an instability of homogenous magnetized matter towards phase separation.

For large magnetic fields, the effects of anisotropy become important, in particular the parallel and perpendicular components of pressure differ substantially. We show the variations of P_{\parallel} and P_{\perp} with B within the RP and bag models at $n = 6n_0$ in Fig. 2b. We note that below $B = 3 \times 10^{18} \text{ G}$, both P_{\parallel} and P_{\perp} are practically equal to the pressure of matter in absence of magnetic field. Hence, we conclude that for the SQM the effect of magnetic field is not significant below $B \sim 10^{18} \text{ G}$ in the framework of our current modes. For larger fields P_{\parallel} increases whereas P_{\perp} decreases in both models of SQM. For large enough fields P_{\perp} becomes negative starting from some critical value of B ; this critical value is almost the same in both models. We now recall that for very large magnetic field $P_{\perp} \rightarrow 0$ in the models without confinement [14, 15]. We see that the addition of the confining potential provides additional “attraction” inside the SQM and its effect becomes more transparent at larger B .

4. Conclusions

We have found that above a certain critical field value $B_{cr} \sim 10^{18} \text{ G}$ the hyperonic matter may become unstable. The instability arises due to negative contribution of the field pressure to the pressure of matter. The details of the onset of instability depend on the assumed central field value B_c as well as the parameterization of the field profile. The instability puts a natural upper bound on the possible central magnetic field of a neutron star.

We find significant differences between the equation of state of the strange quark matter

predicted by the RP and the bag models. This is due to the intrinsic momentum-dependent interaction between quarks in the RP model, which mimics the one-gluon-exchange interaction of the QCD. Specifically, we find that the thermodynamic pressure in the RP model is more sensitive to baryon density when the magnetic field is strong. The de Haas-van Alfvén type oscillations in the transverse pressure P_{\perp} are much more pronounced in the RP model than in the MIT bag model.

Furthermore, we find that the presence of a confining potential, modeled either in terms of the Richardson potential or the MIT bag, suppresses the pressure components P_{\parallel} and P_{\perp} and, at large B , the anisotropy in the equation of state. The splitting between the longitudinal pressure P_{\parallel} and the transverse pressure P_{\perp} was found to be weaker than that in free (non-interacting) strange quark matter. This underlines the importance of taking into account the confining potential in studies of strongly magnetic strange quark matter in cores of neutron stars and in strange stars. It remains an interesting task to explore the effects of the confining potential on the structure and geometry of strongly magnetized stars.

Acknowledgments

The author acknowledges the support of the Alexander von Humboldt Foundation.

References

- [1] Usov V V 1992 *Nature* **357** 472
- [2] Thompson C and Duncan R C 1995 *Mon. Not. Roy. Astron. Soc.* **275** 255
- [3] Thompson C and Duncan R C 1996 *Astro. Phys. J.* **473** 322
- [4] Chodos A, Jaffe R L, Johnson K, Thorn C B and Weisskopf V F 1974 *Phys. Rev. D* **9** 3471
- [5] Nambu Y and Jona-Lasinio G 1961 *Phys. Rev.* **124** 246
- [6] Nambu Y and Jona-Lasinio G 1961 *Phys. Rev.* **122** 345
- [7] Dey M, Bombaci I, Dey J, Ray S and Samanta B C 1998 *Phys. Lett. B* **438** 123
- [8] Richardson J L 1979 *Phys. Lett. B* **82** 272
- [9] Walecka J D 1974 *Ann. Phys.* **83** 491
- [10] Glendenning N K 1987 *Zeitschrift für Physik A Hadrons and Nuclei* **327** 295
- [11] Sinha M, Mukhopadhyay B and Sedrakian A 2013 *Nucl. Phys. A* **898** 43
- [12] Bandyopadhyay D, Chakrabarty S and Pal S 1997 *Phys. Rev. Lett.* **79** 2176–2179
- [13] Sinha M, Huang X G and Sedrakian A 2013 *Phys. Rev. D* **88** 025008
- [14] Huang X G, Huang M, Rischke D H and Sedrakian A 2010 *Phys. Rev. D* **81** 045015
- [15] Dexheimer V, Negreiros R and Schramm S 2012 *Euro. Phys. J. A* **48** 189